© 2018. Published by The Company of Biologists Ltd | Journal of Cell Science (2018) 131, jcs213462. doi:10.1242/jcs.213462

RESEARCH ARTICLE

Spatio-temporal MAPK dynamics mediate cell behavior coordination during fungal somatic cell fusion

Antonio Serrano[1], Julia Illgen[1], Ulrike Brandt[1], Nils Thieme[1,*], Anja Letz[1], Alexander Lichius[2], Nick D. Read[3] and André Fleißner[1,‡]

ABSTRACT

Mitogen-activated protein kinases (MAPKs) are conserved regulators of proliferation, differentiation and adaptation in eukaryotic cells. Their activity often involves changes in their subcellular localization, indicating an important role for these spatio-temporal dynamics in signal transmission. A striking model illustrating these dynamics is somatic cell fusion in *Neurospora crassa*. Germinating spores of this fungus rapidly alternate between signal sending and receiving, thereby establishing a cell-cell dialog, which involves the alternating membrane recruitment of the MAPK MAK-2 in both fusion partners. Here, we show that the dynamic translocation of MAK-2 is essential for coordinating the behavior of the fusion partners before physical contact. The activation and function of the kinase strongly correlate with its subcellular localization, indicating a crucial contribution of the MAPK dynamics in establishing regulatory feedback loops, which establish the oscillatory signaling mode. In addition, we provide evidence that MAK-2 not only contributes to cell-cell communication, but also mediates cell-cell fusion. The MAK-2 dynamics significantly differ between these two processes, suggesting a role for the MAPK in switching of the cellular program between communication and fusion.

KEY WORDS: MAPK, Cell fusion, Directed growth, Cell communication

INTRODUCTION

Mitogen-activated protein kinase (MAPK) cascades are highly conserved eukaryotic signaling circuits that translate extracellular signals in a plethora of crucial cellular processes, including cell-cell communication, cell cycle progression, differentiation, stress adaptation or apoptosis. The structural and functional core of these signaling pathways usually comprises a three-tiered module of hierarchical kinases, which consecutively activate each other via phosphorylation (Cargnello and Roux, 2011). The processes governed by these central signaling hubs mostly outnumber the different MAPKs of a given cell, indicating the need for their fine-tuned activation and inactivation within differently composed molecular networks (Keshet and Seger, 2010). The last three decades have seen much progress in understanding the structural composition of MAPK cascades, including the identification of upstream activating factors, downstream targets and important regulatory components, such as scaffolding proteins and inactivating phosphatases. The contribution of the subcellular spatio-temporal dynamics of MAPKs to their regulation is, however, just beginning to unfold (Atay and Skotheim, 2017).

Both MAPK activation and function commonly require translocation of the kinases within the cell and between different cellular compartments (Wainstein and Seger, 2016). Activation often occurs at the cell surface followed by translocation of the MAPK into the nucleus, where it activates specific transcription factors and is inactivated by phosphatases. One of the most intensively studied MAPK cascades is the pheromone response pathway of baker's yeast (*Saccharomyces cerevisiae*). Here, the MAPK Fus3, its upstream activators Ste7 and Ste11, and the scaffold protein Ste5 are recruited to the plasma membrane in response to signaling initiation by mating pheromone (Good et al., 2009; van Drogen et al., 2001). Activated Fus3 regulates the polarity and directed growth of the forming cellular protuberance, the shmoo, but also translocates into the nucleus, thereby adapting the gene expression profile for the mating reaction (Matheos et al., 2004; Merlini et al., 2013). Similarly, in human cells, nuclear translocation of the ERK1 or ERK2 (ERK1/2) MAPK is essential for the induction of cell proliferation. Prevention of this process with specific inhibitors is nowadays used for combatting various ERK1/2-related cancers, highlighting the importance of understanding the subcellular dynamics of MAPKs (Plotnikov et al., 2015).

The subcellular localization of MAPK activation can strongly influence its signal intensity and propagation. For example, spatio-temporal rewiring of the signaling cascade can serve as a prerequisite for activation, thereby providing a higher order of specificity. In yeast mating, membrane recruitment of the Fus3 module is thought to locally concentrate the interacting activating factors, leading to an increased efficiency of signal transduction (Lamson et al., 2006). Consistent with this notion, arresting Fus3 in the nucleus and, thereby, preventing its translocation to the plasma membrane results in significantly reduced activation (Chen et al., 2010). The spatial partitioning of MAPK-activating factors at the tip of the mating projection and MAPK-deactivating phosphatases in the cytoplasm creates a gradient of activated MAPKs, which ensures spatially constrained signaling from the growing cell tip (Maeder et al., 2007). The specific localization of MAPK activation can also modulate the signaling characteristics, for example to give either a switch-like or a graded cellular response. For example, activation of RAF, the MAPK upstream of ERK, in the cytoplasm yields a response proportional to the signal input level, whereas activation at the plasma membrane generates a maximal output response (Harding et al., 2005). In *S. cerevisiae*, different subcellular dynamic patterns of Fus3 activation correlate with the

[1]Institut für Genetik, Technische Universität Braunschweig, Spielmannstraße 7, 38106 Braunschweig, Germany. [2]Institute of Microbiology, University of Innsbruck, 6020 Innsbruck, Austria. [3]Manchester Fungal Infection Group, Division of Infection, Immunity and Respiratory Medicine, University of Manchester, Manchester M13 9NT, UK.
*Present address: HFM, TUM School of Life Sciences Weihenstephan, Technical University of Munich, Freising D-85354, Germany.

‡Author for correspondence (a.fleissner@tu-bs.de)

A.L., 0000-0002-2323-7583; A.F., 0000-0001-5841-3199

Received 22 November 2017; Accepted 20 March 2018

Journal of Cell Science (2018) 131, jcs213462. doi:10.1242/jcs.213462

differentiation into distinct cell fates, such that sustained Fus3 activation results in growth arrest and shmoo formation, whereas pulsatile activation dynamics is observed during elongated cell growth (Li et al., 2017). In addition, changes in MAPK activity patterns also mediate the different phases of the mating process. Submaximal activity is maintained during early cell cycle arrest, whereas an increase and rapid loss of activity are associated with cell polarization and fusion of the mating partners (Conlon et al., 2016).

Many key questions concerning these crucial subcellular dynamics and their role in signal transmission remain unanswered, including what the mechanism and function of membrane recruitment and release is, what the consequences of MAPK accumulation in a specific cellular compartment are for the crosstalk with other pathways, or what the subcellular routes of individual kinase molecules are from their activation, interaction with their targets and subsequent inactivation.

A unique example of a cellular process involving highly regulated, rapid spatio-temporal MAPK dynamics is somatic cell fusion in *Neurospora crassa*, a long-standing model organism in genetics and cell biology. Vegetative spores (conidia) of this fungus undergo mutual attraction and fusion briefly after germination. Consecutive fusion events merge numerous individuals into one syncytial unit, which further develops into the mycelial fungal colony (Glass et al., 2004; Serrano et al., 2017). During the positive tropic interaction of two germinating spores (called 'germlings'), both cells rapidly alternate between two physiological stages, indicated by the oscillating recruitment of the MAK-2 MAPK module to the plasma membrane of the growing cell tips. MAK-2 is homologous to Fus3 of baker's yeast and is essential for the mutual attraction of the fusion cells (Pandey et al., 2004). Strikingly, plasma membrane recruitment and release of the kinase module occurs in exact antiphase in the two cells, with one phase lasting between 6 and 12 min. In addition, within each individual cell, the kinase recruitment alternates with translocation of the fungal-specific, cytoplasmic SO protein to the plasma membrane (Fleissner et al., 2009; Fleißner and Herzog, 2016). Taken together, these observations indicate that the two cells coordinate their behavior over a spatial distance before physical contact. The current working model suggests that the two interacting cells take turns to send and receive signals, thereby establishing a 'cell-cell dialog'. Interrupting signal transduction in just one of the two partners, e.g. by MAK-2 inhibition, also terminates signaling in the second cell, indicating that the 'cell-cell dialog' mechanism is not cell autonomous and requires ongoing coordination of the two fusion cells (Fleissner et al., 2009). Mathematical modeling has suggested that an intricate signaling circuit composed of positive and negative feedback loops mediates this cellular interaction, allowing the two interacting cells to employ the same signaling ligand and receptor system (Goryachev et al., 2012). Similar to what occurs in yeast mating, MAK-2 seems to function in two different branches during germling fusion. First, it controls gene regulation via the Ste12-homologous transcription factor PP-1, and, second, it guides the growth of the two fusion partners towards each other (Leeder et al., 2013). Recent years have seen much progress in identifying numerous additional factors essential for germling fusion and the 'cell-cell dialog' mechanism (Fleißner and Serrano, 2015; Leeder et al., 2011). However, the function of the observed rapid MAPK dynamics remain to be elucidated.

Here we show, by manipulating the spatio-temporal dynamics of MAK-2, that its alternating membrane recruitment is essential for the coordination of the cellular behavior. The phosphorylation state and kinase activity of MAK-2 strongly correlate with its subcellular localization, emphasizing the importance of the subcellular dynamics for its regulation. Interestingly, the presence of the kinase at the plasma membrane prevents recruitment of the SO protein, providing a novel insight into the mechanistic basis of the coordinated oscillatory cellular behavior. In addition, we provide evidence that MAK-2 spatio-temporal dynamics are essential not only for cell-cell communication and directed growth, but also after physical contact of the two interacting partners during cell-cell fusion.

RESULTS

Adapting a protein membrane-tethering system for *N. crassa*

A striking feature of germling fusion is the highly coordinated oscillatory recruitment of the MAK-2 MAPK module to the plasma membrane of cell fusion tips (Fleissner et al., 2009). To test the role of this dynamic behavior, we sought to disrupt the translocation of MAK-2 within the cell by tethering it to the plasma membrane. Because no molecular tool for this manipulation has been established for *N. crassa*, we tested two different strategies by using green fluorescent protein (GFP) as a reporter. First, a commercially available construct consisting of *egfp* fused to a sequence encoding the CAAX box-containing C-terminus of the human c-Ha-Ras (GFP-F) was expressed in the wild-type background, resulting in strain 37. Second, *sgfp* (encoding superfolder GFP) was fused to the sequence encoding the CAAX box-containing C-terminal 20 amino acids of BAND (*ras-1*, NCU08823) of *N. crassa* and was also expressed in the wild type, resulting in strain 800 (Fig. S1A). In mammalian cells, GFP-F is efficiently recruited to the plasma membrane, whereas BAND of *N. crassa* is predicted to localize to this cellular compartment (Belden et al., 2007). Fluorescence microscopy of strains 37 and 800 revealed that tagging with the mammalian CAAX box resulted in inefficient plasma membrane recruitment of GFP. Fluorescence was detected in the cytoplasm and within the vacuolar lumen (Fig. S1B). In contrast, GFP fused to the fungal BAND sequence strongly accumulated at the plasma membrane, septa and vacuoles (Fig. S1C). Expression of both constructs did not visibly influence the phenotype of the fungus (Fig. S1D). In summary, the fungal BAND CAAX box represents a robust tool for directing proteins to the plasma membrane in *N. crassa*, whereas the mammalian signal seems to be only poorly recognized in fungal cells.

Subcellular spatiotemporal dynamics of MAK-2 are essential during vegetative cell fusion

After establishing the membrane-tethering tool for *N. crassa*, we employed it to disrupt subcellular MAK-2 dynamics. The 3′-end of the *mak-2* open reading frame was fused to the GFP–CAAX-encoding sequence. The resulting construct was expressed under control of its native promoter or the *tef-1* promoter, which is routinely used in subcellular localization studies in *N. crassa* (Berepiki et al., 2010). In addition, a construct carrying a mutation in the CAAX box-encoding sequence, which results in a replacement of the critical cysteine with a serine residue (SAAX), was expressed under the native and the *tef-1* promoter and used as a control. The four constructs were expressed in the Δ*mak-2* gene knockout mutant, resulting in strains 642 (CAAX, native promoter), 640 (CAAX, *tef-1* promoter), 404 (SAAX, native promoter) and 381 (SAAX, *tef-1* promoter). Although the control strains exhibited full complementation of the macroscopic Δ*mak-2* phenotype, both strains expressing the CAAX box proteins still appeared to have the

Journal of Cell Science (2018) 131, jcs213462. doi:10.1242/jcs.213462

mutant phenotype (Fig. 1A). Fluorescence microscopy imaging revealed that, in the control strains, MAK-2–GFP–SAAX was mostly cytoplasmic and nuclear in hyphae and conidial germlings, whereas the overexpressed CAAX box variant was efficiently tethered to the plasma membrane and no nuclear localization was observed (Fig. 1B). The native expression of the CAAX box-tagged MAK-2–GFP (642) showed a very weak fluorescence signal, and no unambiguous localization was possible. To test the subcellular

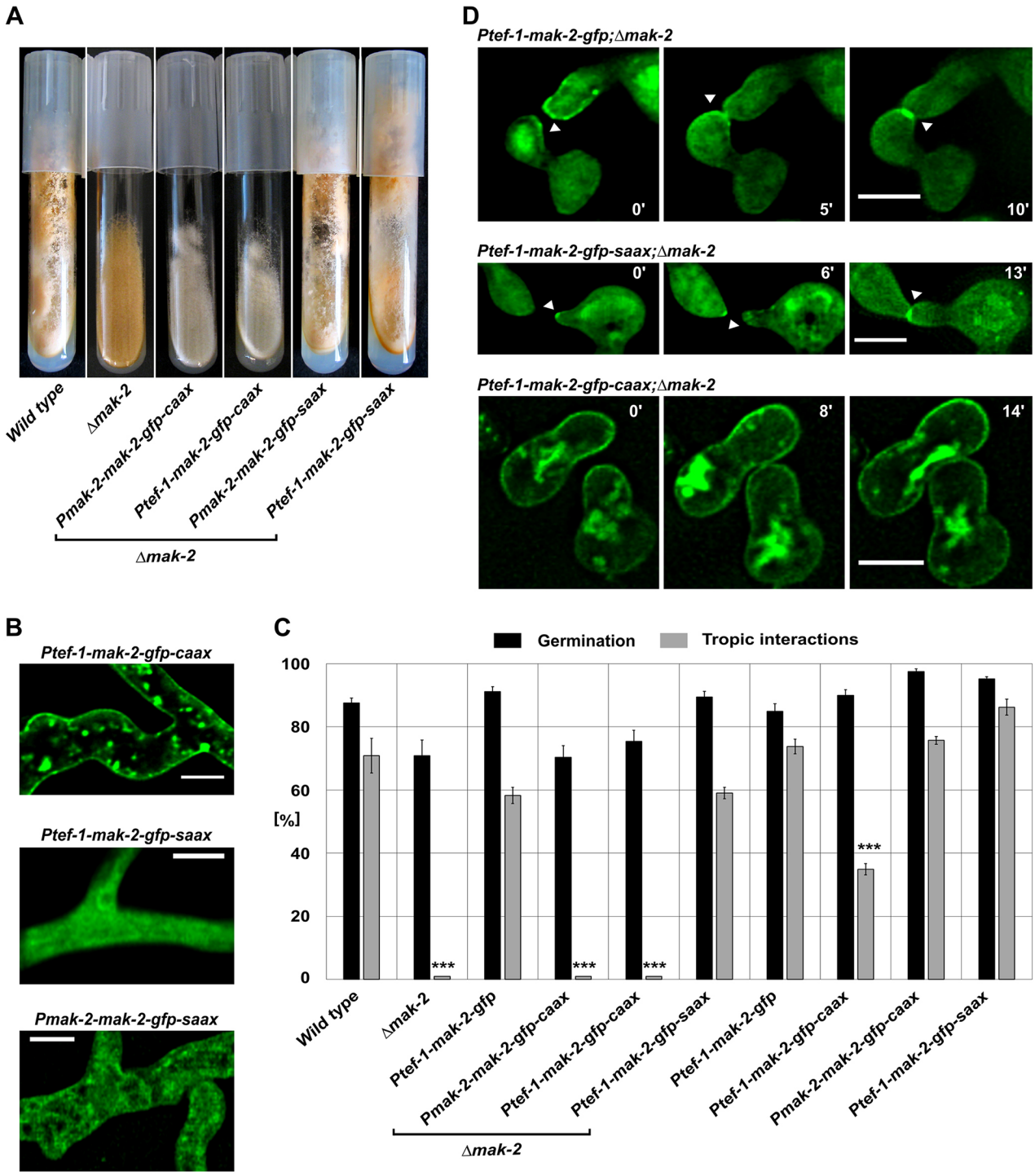

Fig. 1. Membrane tethering of MAK-2 does not complement the phenotypic defects of the Δ*mak-2* mutant. (A) Macroscopic phenotypes of Δ*mak-2* strains transformed with CAAX constructs, strains 642 (*mak-2::hph;Pmak-2–mak-2–gfp–caax*) and 640 (*mak-2::hph;Ptef-1–mak-2–gfp–caax*), and the SAAX control, with strains 404 (*mak-2::hph;Pmak-2–mak-2–gfp–saax*) and 381 (*mak-2::hph;Ptef-1–mak-2–gfp–caax*). (B) Subcellular localization of the MAK-2 construct fused to GFP–CAAX (640) and GFP–SAAX (strains 404 and 381). Comparable observations were made for multiple samples ($n \geq 30$). (C) Quantitative analysis of tropic interactions and germination of tested strains: wild type (FGSC 2489), Δ*mak-2*, 633 (*mak-2::hph;Ptef-1–mak-2–gfp*), 642, 640, 381, 665 (*Ptef-1–mak-2–gfp*), 267 (*Ptef-1–mak-2–gfp–caax*), 353 (*Pmak-2–mak-2–gfp–caax*) and 361 (*Ptef-1–mak-2–gfp–saax*). Results are means±s.d. ($n \approx 100$). ***$P<0.01$ (compared with wild type). (D) Time course of MAK-2-tagged constructs with GFP–SAAX (381), GFP (633) and GFP–CAAX (640). Scale bars: 5 µm. (note that the different diameters of the interacting germ tubes reflect the normal variation of these structures in *N. crassa*).

Journal of Cell Science (2018) 131, jcs213462. doi:10.1242/jcs.213462

dynamics of the different MAK-2 variants, germling fusion assays were conducted. Although the control strains exhibited cell-cell interaction rates comparable to those of the wild type, no positive tropic interactions were observed in the Δ*mak-2* knockout mutant or the strains carrying the CAAX constructs (Fig. 1C). The control construct was recruited to the plasma membrane of fusion tips in the characteristic coordinated oscillatory manner, whereas the CAAX constructs remained stable at the plasma membrane (Fig. 1D). Taken together, these observations indicate that the spatial subcellular dynamics of MAK-2 are essential for its functioning in mediating cell-cell communication and fusion, but also for general growth and development.

After determining the essential function of the oscillatory MAK-2 recruitment, we asked whether the permanent presence of the kinase at the plasma membrane disturbs this process in a wild-type background. The *Ptef-1–mak-2–gfp–caax* construct and the respective control constructs (*Ptef-1–mak-2–gfp* and *Ptef-1–mak-2–gfp–saax*) were transformed into the wild-type background, and the resulting transformants were analyzed by brightfield and fluorescence microscopy. Although in the controls, germlings (strains 665 and 361) underwent wild-type-like interactions and the GFP construct was recruited in the normal oscillatory manner, interactions in the isolate carrying the CAAX construct (strain 267) were significantly reduced (Fig. 1C). This observation suggested that the permanent presence of MAK-2 at the plasma membrane imposes a dominant-negative effect on germling fusion. In addition, the macroscopic development of the respective isolates is also impaired (Fig. S1E-G).

Tethering of MAK-2 to the plasma membrane results in its hyperphosphorylation through upstream kinases

In order to test whether the subcellular localization of MAK-2 influences its activation, the phosphorylation of the MAPK was determined by western blot analysis. The strains carrying the *mak-2–gfp–caax* and *mak-2–gfp–saax* constructs expressed from the native and *tef-1* promoter (strains 642, 640, 404 and 381, respectively) were tested. *Mak-2–gfp*-expressing strains were used as controls (P611-3 and 633). All isolates were cultivated in shaking liquid medium. Under these conditions, cell-cell interactions and fusions are highly reduced, and MAK-2 exhibits only basal phosphorylation in the wild type. The western blot analysis revealed a strong hyperphosphorylation of the CAAX variants, whereas the SAAX sequence had no influence on the phosphorylation level (Fig. 2A). Control hybridization with an anti-GFP antibody revealed that the CAAX sequence appeared to have a negative impact on protein stability. In all CAAX samples, the GFP-derived signals were reduced compared with the *mak-2–gfp* or *mak-2–gfp–saax* strains (Fig. 2B). However, the expression of the CAAX construct under control of the *tef-1* promoter reached the level of wild-type *mak-2* expression, but no complementation of the Δ*mak-2* phenotype was observed. Taken together, these data suggest that the observed defects are due to the disruption of MAK-2 dynamics rather than reduced protein levels.

To test whether the observed hyperphosphorylation is mediated by interactions within the MAK-2 module, the overexpressed CAAX constructs were expressed in knockout mutants for the two upstream kinases MEK-2 and NRC-1 (the resulting strains are 384 and 670, respectively). In both isolates, the kinase was again efficiently recruited to the plasma membrane (Fig. S2A,B). The presence of this construct had no positive influence on the cell-cell communication deficiency of the knockout mutants (Fig. S2C). Western blot analysis revealed that, in the absence of MEK-2 or NRC-1, no phosphorylation of MAK-2 occurs independently of its subcellular localization (Fig. 2C,D). Similarly, the lack of HAM-5, a scaffolding protein for the MAK-2 module, caused a reduced phosphorylation of the membrane-tethered MAPK (Fig. 2C,D). Taken together, these data indicate that changing the localization of MAK-2 towards the plasma membrane results in its strong activation via the upstream kinases, even under conditions that usually do not promote activation of the MAPK module. When tested under conditions that promote germling fusion, strains carrying the membrane-tethered MAK-2 also showed an overall increased phosphorylation of the MAPK (Fig. S2D). Although the MAK-2–GFP–CAAX constructs stably remained at the plasma membrane, the MAK-2–GFP control exhibited the usual dynamic localization (Fig. S2E–G). Taken together, these observations strongly suggest a correlation between the relative amount of membrane-associated MAK-2 and the level of overall phosphorylation.

Tethering of the upstream kinase MEK-2 to the plasma membrane results in only a partial loss of function

During wild-type interactions, MAK-2 is translocated into the nuclei, where it is thought to target transcription factors, such as PP-1 (Li et al., 2005). Membrane tethering excludes the kinase from this organelle, which in part might explain the observed loss of function of the MAK-2–GFP–CAAX constructs. Activation of MAPKs by their upstream kinases usually occurs at the membrane or in the cytoplasm (Cargnello and Roux, 2011; Harding et al., 2005). We therefore hypothesized that membrane tethering of MEK-2 should still allow its function to some extent. To test this hypothesis, a MEK-2–GFP–CAAX construct was expressed in the Δ*mek-2* mutant (*his-3*;Δ*mek-2*) and in the wild type, resulting in strains 618 and 330, respectively. Strains carrying the MEK-2–GFP–SAAX and MEK-2–GFP constructs in the same mutant and wild-type background were used as controls (423, 406 and 549). As predicted, the protein linked to the CAAX motif was localized at the plasma membrane (Fig. 3A), whereas the controls showed the typical subcellular dynamic localization (Fig. S3A,B). Tethering of MEK-2 to the plasma membrane had no effect on MAK-2 phosphorylation, suggesting that this signal transmission step can fully take place at the membrane (Fig. S3C). Furthermore, germling interactions did not improve in the Δ*mek-2* background isolate (Fig. 3B), and a significant number of cells exhibited polarity defects, indicated by extended apolar growth (Movie 1). It was therefore unclear whether the interaction defects were caused by trapping the kinase at the membrane or whether they were a secondary effect of the disturbed polarity. Recent studies have revealed that the oscillating MAK-2 recruitment also mediates fusion between hyphae in the inner parts of mature mycelial colonies of *N. crassa*, suggesting that germling and hyphal fusion share a common molecular mechanism (Jonkers et al., 2014). Hyphal fusion is absent in Δ*mek-2*, but is restored in the presence of membrane-anchored MEK-2–GFP–CAAX, albeit at a lower frequency than in the wild type (Fig. S3D). This finding suggests that the fusion-related cellular interaction does not require wild-type-like spatial dynamics of the upstream kinase MEK-2.

Defects in the sexual development of the Δ*mek-2* mutants were also complemented by the membrane-tethered version of MEK-2. Sexual spores carrying the Δ*mek-2* mutation are non-viable. This so-called ascospore lethality was complemented by the expression of the membrane-tethered version of MEK-2 (Fig. 3C). Interestingly, however, fruiting bodies (perithecia) formed in crosses using strain 279 as the female partner were misshaped, and the orientation of

Journal of Cell Science (2018) 131, jcs213462. doi:10.1242/jcs.213462

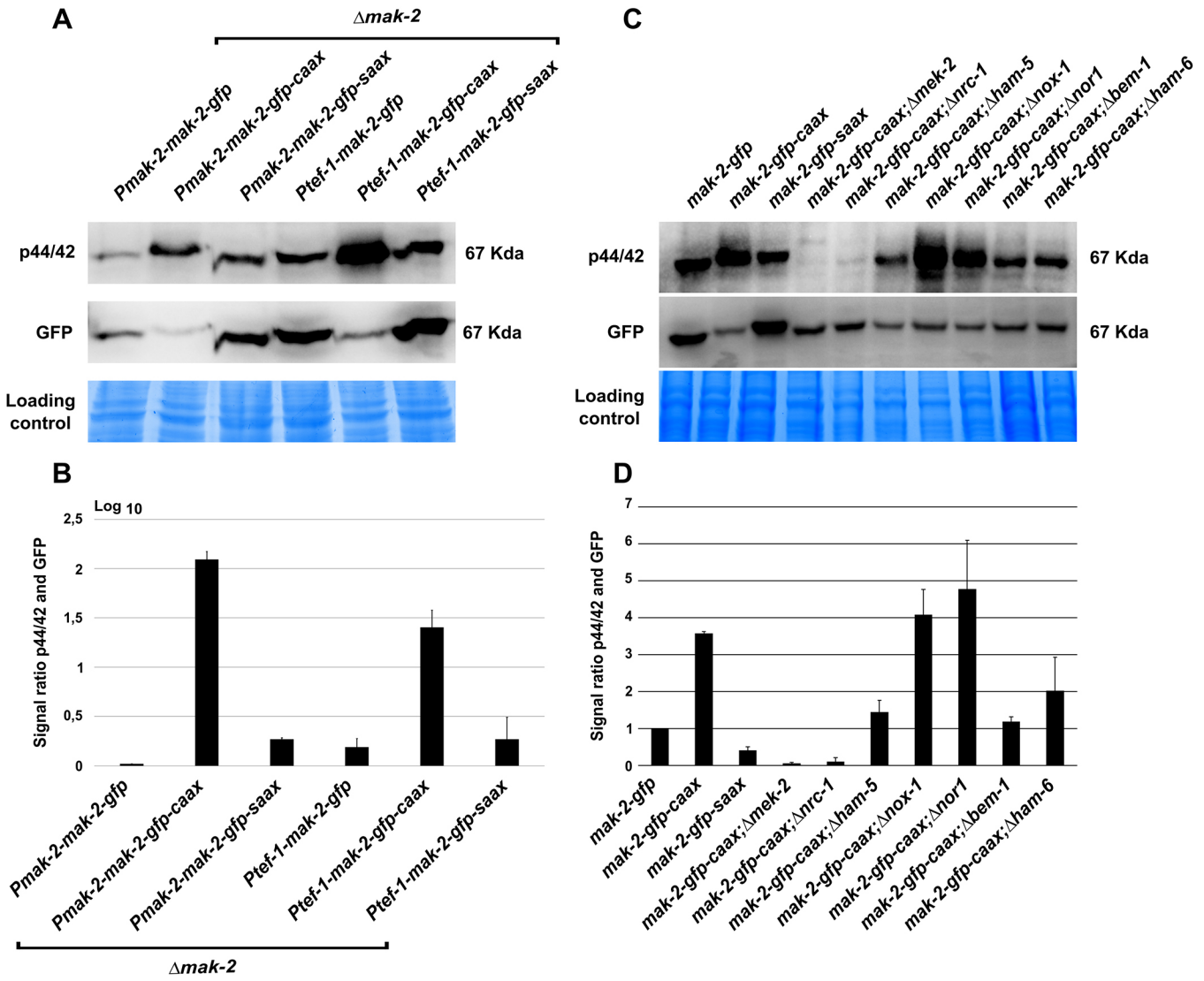

Fig. 2. Membrane tethering results in increased phosphorylation of MAK-2 (A) Phospho-western blot analysis. The order of the lanes are: strain P611-3 (*mak-2::hph; his3::Pmak-2–mak-2–gfp*), strain 642 (*mak-2::hph; his3::Pmak-2–mak-2–gfp–caax*), strain 404 (*mak-2::hph; his3::Pmak-2–mak-2–gfp–saax*), strain 633 (*mak-2::hph; his3::Ptef-1–mak-2–gfp*), strain 640 (*mak-2::hph; his3::Ptef-1–mak-2–gfp–caax*) and strain 381 (*mak-2::hph; his3::Ptef-1–mak-2–gfp–saax*). (B) Analyses of the ratio between the phosphorylation and GFP signals for every lane. Results are means±s.d. (*n*=3). (C) Western blot analysis detecting MAK-2 phosphorylation and GFP of the following strains: 665 (*his3::Ptef-1–mak-2–gfp*), 267 (*his3::Ptef-1–mak-2–gfp–caax*), 361 (*his3::Ptef-1–mak-2–gfp–saax*), 384 (*mek-2::hph;his3::Ptef-1–mak-2–gfp–caax*), 670 (*nrc-1::hph;his3::Ptef-1–mak-2–gfp–caax*), 770 (*ham-5::hph;his3::Ptef-1–mak-2–gfp–caax*), 723 (*nox-1::hph;his3::Ptef-1–mak-2–gfp–caax*), 719 (*nor-1::hph,his3::Ptef-1–mak-2–gfp–caax*), 569 (*bem-1::hph;his3::Ptef-1–mak-2–gfp–caax*) and 773 (*ham-6::hph;his3::Ptef-1–mak-2–gfp–caax*). (D) Quantification of the ratio between the phosphorylation signal and GFP signal. Results are means±s.d. (*n*=3).

their typical beaks (perithecial necks) was disturbed (Fig. 3D,E). Frequently, fruiting bodies with more than just one beak developed. Although, in wild type, beaks mostly grow perpendicular to the agar surface, their orientation was mostly random in the mutant, frequently resulting in spore discharge into the growth medium (Fig. 3E,F). Crosses with strain 279 as the male partner produced normal-shaped fruiting bodies (Fig. 3F), indicating a female-specific function of normal MEK-2 dynamics in fruiting body formation.

Membrane tethering of activated MAK-2 disrupts SO dynamics

One of the most striking features of the ‘cell-cell dialog’ mode of communication is the highly coordinated alternating recruitment of MAK-2 and SO to the plasma membrane. Although both proteins are recruited to the same cellular region into similar structures, they are not associated with the plasma membrane at the same time and do not colocalize before cell-cell contact is established. We therefore set out to analyze the subcellular dynamics of SO during germling fusion when MAK-2 is permanently tethered to the plasma membrane. MAK-2–GFP–CAAX and dsRed–SO were expressed in a heterokaryon created by vegetative fusion of strains 267 and 843, and germlings were analyzed by brightfield and fluorescence microscopy. As observed above, the wild-type background of these germlings allowed cell-cell interactions, albeit at a significantly reduced frequency. Although the cells exhibited a clear dsRed–SO fluorescent signal, no oscillatory recruitment of the fusion construct to the plasma membrane was

Journal of Cell Science (2018) 131, jcs213462. doi:10.1242/jcs.213462

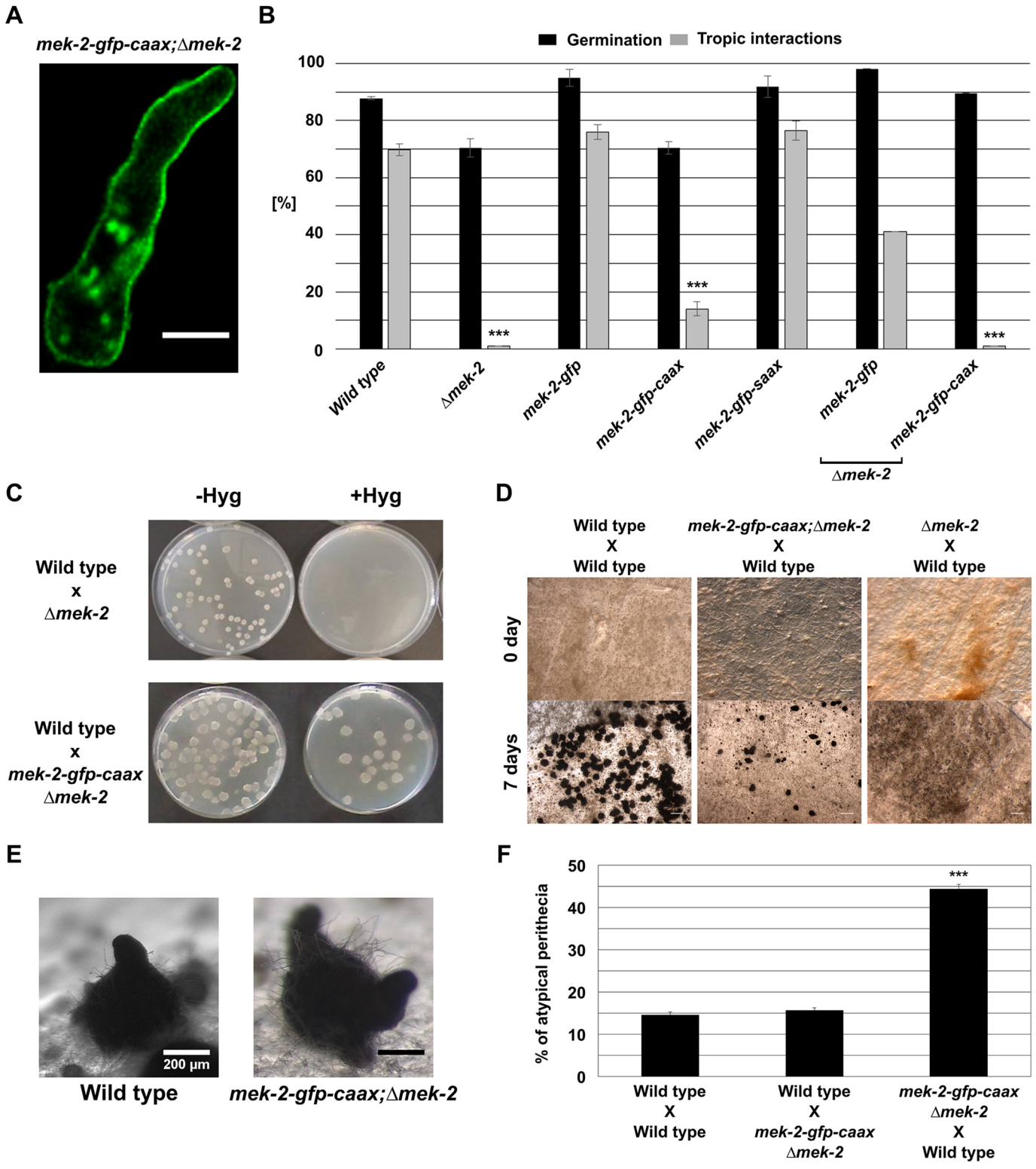

Fig. 3. Membrane-tethered MEK-2 partially complements the developmental defects of the Δ*mek-2* mutant. (A) The C-terminal fusion of a CAAX box domain to MEK-2 induces membrane tethering of the protein. Comparable observations were made for multiple samples (n=15). (B) Quantification of tropic interactions and germination of the following strains: wild type (FGSC 2489), Δ*mek-2*, 406 (*his3::Ptef-1–mek-2–gfp*), 330 (*his3::Ptef-1–mek-2–gfp–caax*), 549 (*his3::Ptef-1–mek-2–gfp–saax*), 423 (*mek-2::hph;his3::Ptef-1–mek-2–gfp*) and 618 (*mek-2::hph;his3::Ptef-1–mek-2–gfp–caax*). Results are means±s.d. (n≈100). ***P<0.01 (compared with wild type). (C) Viability test of progeny from the crosses. Progeny carrying the Δ*mek-2* mutation is hygromycin (Hyg) resistant but inviable. The presence of MEK-2–GFP–CAAX in strain 279 (*mek-2::hph;his3::Pmek-2–mek-2–gfp–caax*) complements this lethality. Comparable observations were made for three different sexual crosses. (D) Sexual crosses of the strains indicated. The first crossing partner always indicates the female. (E) Fruiting bodies formed after 7 days of incubation. The female crossing partners 279 (*mek-2–gfp–caax;Δmek-2*) and wild type (FGSC 988) are indicated. (F) Quantification of atypical perithecia formed in the crosses depicted in D. Results are means±s.d. (n=16). ***P<0.01 (compared with the wild type X wild type cross). For each strain combination, a total of at least 1500 fruiting bodies were analyzed. Scale bars: 5 µm (A) and 1 mm (D).

Journal of Cell Science (2018) 131, jcs213462. doi:10.1242/jcs.213462

detected during the cellular communication process (n=120). In the control strain expressing MAK-2–GFP, dsRed–SO was recruited in a wild-type-like manner in 88% of cell pairs (n=125). However, the construct strongly accumulated at the side of membrane merger after the cells had established physical contact (Fig. 4A). In the control strain expressing dsRed-SO and GFP–CAAX, the SO dynamics were normal, excluding the possibility of unspecific effects of the presence of a membrane-tethered protein (Fig. 4B). Because MAK-2 is phosphorylated when present at the plasma membrane, we asked whether this activation of the kinase is a prerequisite for preventing SO recruitment. We therefore mutated the two conserved phosphorylation sites of the MAPK (T180A and Y182F), fused the construct to GFP–CAAX and expressed it in the wild type (resulting in strain 797). Although the membrane localization of the construct was comparable to that in the non-mutated version, SO dynamics were not affected by the presence of the construct and exhibited wild-type-like oscillations (Fig. 4C). This observation indicates that only the presence of active MAK-2 negatively controls SO recruitment to the membrane.

As mentioned above, hyphal fusion occurs in the inner part of mature colonies (Movie 2). Because this cell fusion process also employs MAK-2 oscillation, we asked whether SO is also recruited in an alternating manner to the kinase and colocalized both proteins during this process. Consistent with the findings for the MAK-2 module, tip recruitment of SO oscillated, similar to its dynamics in germling fusion, and alternated at the plasma membrane with MAK-2 (Fig. S4A). Comparable to the observations in germlings, the SO membrane association was absent in the presence of phosphorylated membrane-tethered MAK-2 (Fig. S4B).

Taken together these data indicate that, as long as activated MAK-2 is present at the plasma membrane, recruitment of SO is suppressed, which could explain the highly coordinated alternating tip recruitment of these two proteins observed during germling and hyphal fusion.

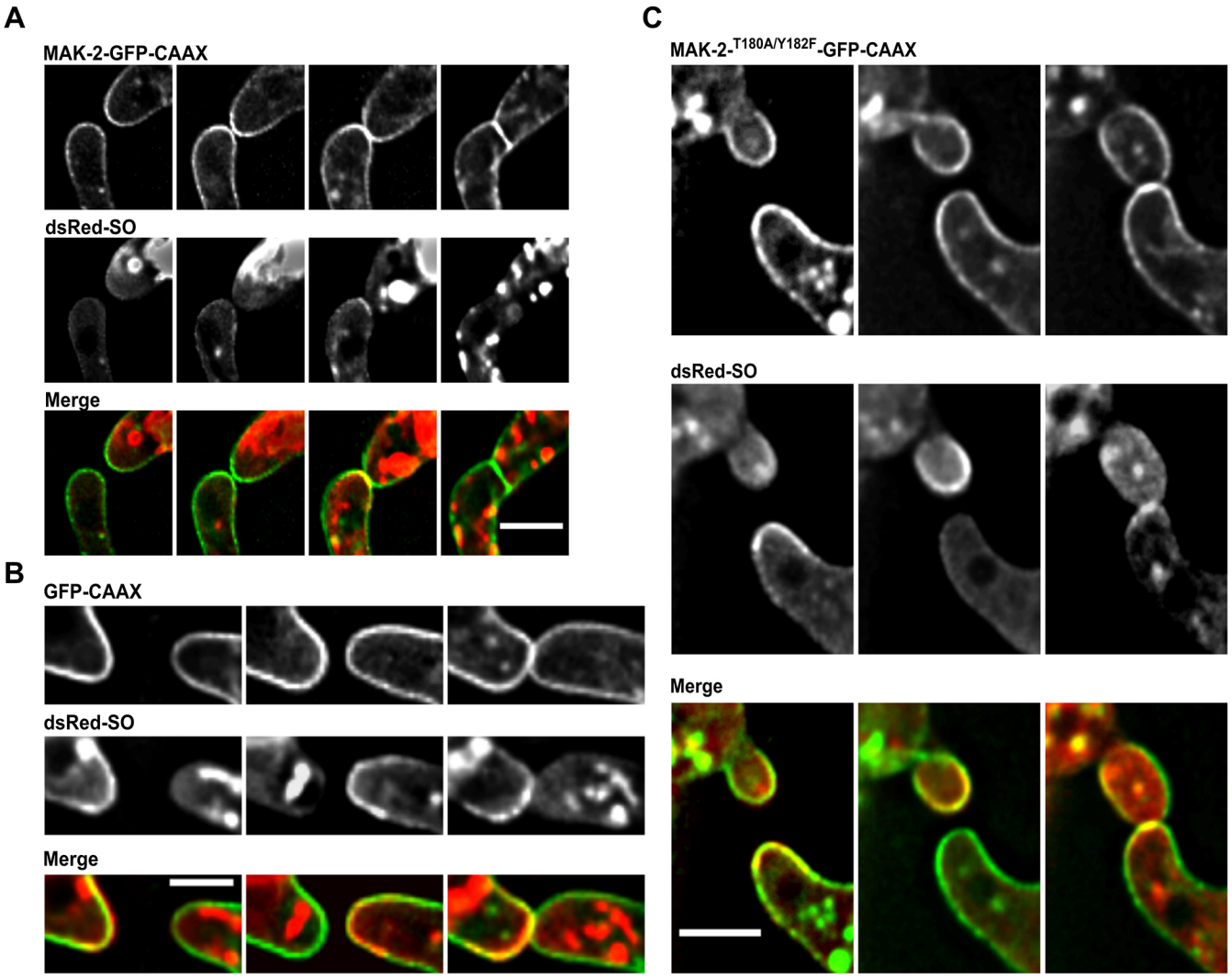

Fig. 4. Membrane recruitment of SO is suppressed in the presence of membrane-tethered MAK-2. (A) Subcellular localization of MAK-2–GFP–CAAX and dsRed–SO in a heterokaryon of strains 267 (*his3::Ptef-1–mak-2–gfp–caax*) and 843 (*his3::Ptef-1–dsRed–SO*). Images were taken at 5 min intervals. Comparable observations were made for multiple samples (n=120). (B) Subcellular localization of GFP–CAAX and dsRed–SO in a heterokaryon of strains 800 (*his3::Ptef-1–gfp–caax*) and 843 (*his3::Ptef-1–dsRed–SO*). Images were taken at 5 min intervals. Comparable observations were made for multiple samples (n=5). (C) Subcellular localization of MAK-2$^{T180A/Y182F}$–GFP–CAAX and dsRed–SO in a heterokaryon of strains 797 (*his3::Ptef-1–mak-2*$^{T180A/Y182F}$*–gfp–caax*) and 843 (*his3::Ptef-1–dsRed–SO*). Images were taken at 5 min intervals. Comparable observations were made for multiple samples (n=5). Scale bars: 5 µm.

Journal of Cell Science (2018) 131, jcs213462. doi:10.1242/jcs.213462

MAK-2 phosphorylation and activity are necessary for the subcellular dynamics during germling and hyphal fusion

The subcellular dynamics of MAPKs not only strongly depend on but also control their own activation and activity. To gain a better understanding of these interrelations we tried to decipher the contribution of phosphorylation and activity by: (1) analyzing the dynamics of a MAK-2 variant with mutated phosphorylation sites, and (2) testing the influence of MAK-2 inhibition on its subcellular localization.

In the first approach, *mak-2* constructs carrying mutations of each individual and both phosphorylation sites and a C-terminal GFP-tag were expressed in the Δ*mak-2* mutant (resulting in strains 607, 610 and 613) and in the wild-type background (resulting in strains 809, 813 and 816) under control of the native *mak-2* promoter. None of the constructs complemented the Δ*mak-2* mutant phenotype, whereas the expression level of the mutant constructs was comparable to that of the wild-type gene (Fig. 5A,B). When expressed in the wild-type background, which allowed cell-cell interactions, the mutated variants MAK-2$^{T180A/Y182F}$ and MAK-2^{Y182F} showed no recruitment to the plasma membrane, indicating that the tyrosine phosphorylation site is essential for MAK-2 dynamic localization (Fig. 5C). In contrast, recruitment of MAK-2 carrying the single mutation of the threonine residue (MAK-2^{T180A}) was still observed, although in an uncoordinated manner, such that at some time points the protein was simultaneously present at both cell tips (Fig. 5C). Interestingly, all three constructs were recruited to the fusion point after the cells made physical contact, indicating that the subcellular dynamics before and after cell-cell contact are differentially regulated.

In the second approach, we followed a chemical genetics strategy to specifically manipulate MAK-2 activity, by creating an ATP analog-sensitive variant (frequently called a 'Shokat allele') (Bishop et al., 2000). In an earlier study, we had already used the inhibitable variant MAK-2^{Q100G} to test the influence of MAK-2 inhibition on SO dynamics. However, this construct was found to be not functional when tagged with GFP. Therefore, the subcellular dynamics of the kinase after its inhibition could not be determined (Fleissner et al., 2009). In the present study, we constructed an

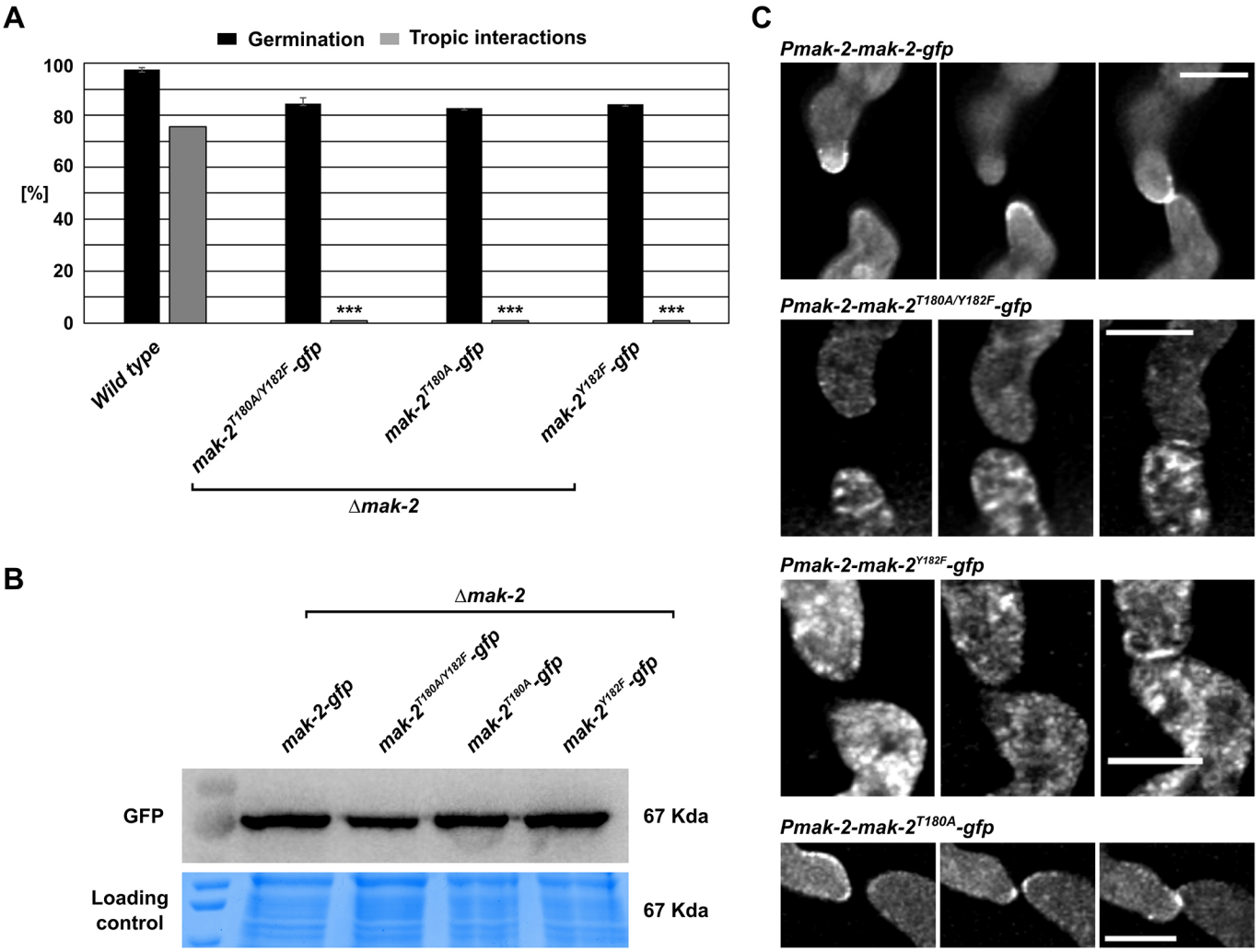

Fig. 5. Subcellular dynamics of different MAK-2 variants carrying mutations at the phosphorylation sites. (A) Quantification of spore germination and tropic interactions of the following strains: wild type (FGSC 2489), 607 (*mak-2::hph;his3::Ptef-1–mak-2$^{T180A/Y182F}$–gfp*), 610 (*mak-2::hph;his3::Ptef-1–mak-2^{T180A}–gfp*) and 613 (*mak-2::hph;Ptef-1–mak-2^{Y182F}–gfp*). Results are means±s.d. (n≥100). ***P<0.01 (compared with wild type). (B) Western blot analyses of the mutated versions of MAK-2. Comparable observations were made for multiple samples (n=3). (C) Localization of *Pmak-2–mak-2–gfp* in strain N1-42, *pmak-2$^{T180A/Y18F}$–gfp* in strain 816, *pmak-2^{T180}–gfp* in strain 813 and *pmak-2^{Y182F}–gfp* in strain 809. Images were taken at 5 min intervals. Scale bars: 5 µm. Comparable observations were made for multiple samples (n≥5 per strain).

Journal of Cell Science (2018) 131, jcs213462. doi:10.1242/jcs.213462

alternative allele, mak-2^{Q100A}, which carried a C-terminal GFP tag, and expressed it in the Δ*mak-2* mutant, resulting in strain 802. The construct fully complemented the Δ*mak-2* cell-cell communication defects in the absence of the inhibitor. Addition of the inhibitor resulted in a Δ*mak-2*-like phenotype (Fig. 6A). Together, these data indicate that this construct was fully functional and allowed us to analyze the dynamics of MAK-2 after inhibition by using fluorescence microscopy. Without the inhibitor, the GFP-tagged kinase underwent wild-type-like dynamics during germling interactions, characterized by the typical oscillatory recruitment to the plasma membrane of the fusion tips (Fig. 6B). Addition of the inhibitor to interacting cells readily suppressed these dynamics, and the cells appeared to be locked in their current stage (Fig. 6C). In the partner without MAK-2 recruitment, the kinase did not accumulate at the plasma membrane for at least 40 min. In the opposite cell, which carried MAK-2 at its cell tip when the inhibitor was added, the protein remained stable at the membrane. It was only after an extended incubation that the GFP signal disappeared from the cell tip. At the same time, accumulation in the nuclei became apparent. To distinguish whether the primary effect of MAK-2 inhibition is the failure of MAK-2 recruitment to the membrane or its release from the membrane, we analyzed fusion pairs consisting of an inhibitable (MAK-2^{Q100A}–GFP-expressing) and a wild-type (MAK-2–GFP-expressing) cell. To discriminate the respective cells, spores carrying the wild-type kinase version were pre-stained with the membrane dye FM4-64. Addition of the inhibitor blocked membrane recruitment of MAK-2^{Q100A}–GFP in the inhibitable cell, as observed before in the homotypic fusion pairings. However, in contrast to the inhibitable variant, wild-type MAK-2–GFP disappeared from the membrane within 4 to 8 min (Fig. 6D). Taken together, these data suggest that MAK-2 activity is essential for both recruitment to and release from the plasma membrane.

The above finding that MAK-2 dynamics are differentially regulated before and after cell-cell contact prompted us to analyze the consequences of MAK-2 inhibition during the final stages of the cell fusion process, when the cell wall is degraded and the plasma membranes merge. Spores from strain N2-01 (MAK-2^{Q100G}) and strain 802 (MAK-2-^{Q100A}–GFP) were mixed. Successful fusion was indicated by the transmission of the fluorescent signal from the GFP-tagged cell into the unlabeled cell. Without the inhibitor, cells interacted and fused in a wild-type-like manner (Fig. 7A). In the presence of the inhibitor, MAK-2^{Q100A}–GFP accumulated at the contact side, but no cytoplasmic mixing occurred (Fig. 7B). Taken together, these data indicate that MAK-2 activity is essential for the dynamic localization during the tropic cell-cell interaction as well as for cell fusion, but is dispensable for the recruitment to the fusion point after cell-cell contact.

BEM-1 is essential for MAK-2 activation in a NOX complex-independent manner

In an earlier study, we showed that the polarity factor BEM-1 promotes vegetative fusion in *N. crassa* and is essential for stable and robust MAK-2 activation (Schürg et al., 2012). Although BEM-1 has a similar function in *S. cerevisiae* mating (Lyons et al., 1996), it is also part of NADPH oxidase (NOX) complexes in filamentous

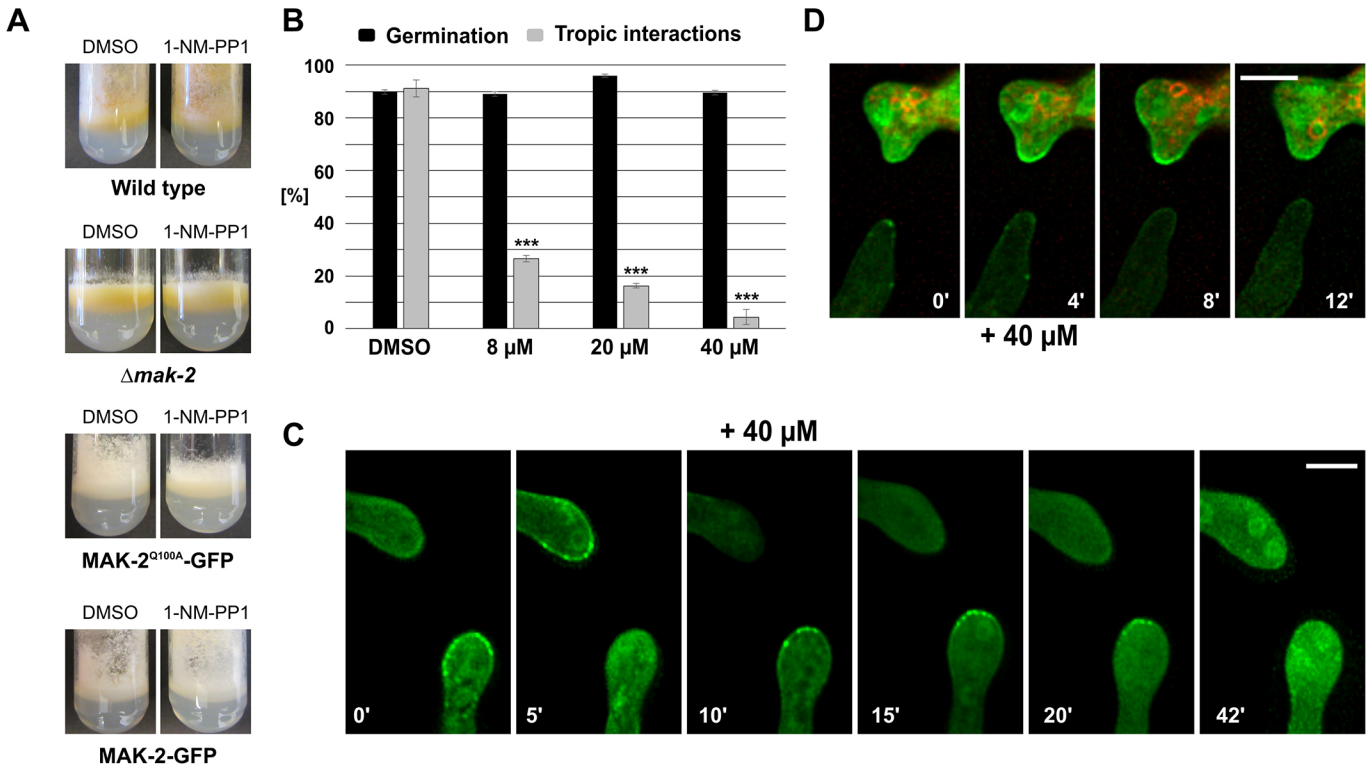

Fig. 6. Effects of the specific inhibition of MAK-2 on growth, development and the subcellular dynamics of the MAPK. (A) Macroscopic phenotype in the presence of DMSO or 1-NM-PP1 (40 µM) of the following strains: wild type (FGSC 2489), Δ*mak-2*, 802 (*mak-2::hph; his3::Ptef-1–mak-2^{Q100A}–gfp*) and 633 (*mak-2::hph;his3::Ptef-1–mak-2–gfp*). Images were taken after 5 days of incubation. (B) Quantification of spore germination and tropic interactions in strain 802 (*mak-2::hph;his3::Ptef-1–mak-2^{Q100A}–gfp*) in the presence of different inhibitor concentrations, 4 h after inoculation. Results are means±s.d. ($n \geq 100$). ***P<0.01 (compared with the DMSO sample). (C) Localization of the analog-sensitive MAK-2 before and after addition of the inhibitor (+40 µM). Comparable observations were made for multiple samples (n=5). (D) Inhibition of a mix of spores between strain 665 (*Ptef-1–mak-2–gfp*) previously incubated with FM4-64 and 802 (*mak-2::hph;Ptef-1–mak-2^{Q100A}–gfp*). Comparable observations were made for multiple samples (n=5). Scale bars: 5 µm.

Journal of Cell Science (2018) 131, jcs213462. doi:10.1242/jcs.213462

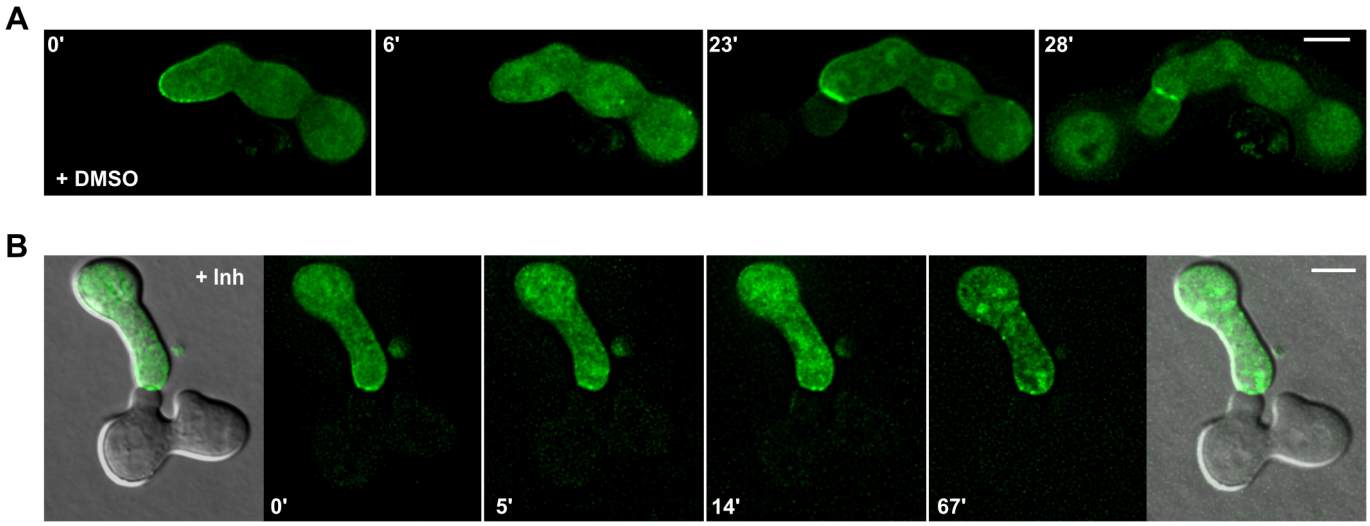

Fig. 7. Effects of MAK-2 inhibition on the cell-cell fusion process. (A) Cell interaction and fusion of spores of strains MAL-1 (*mak-2::hph;his3::pccg-1–mak-2^{Q100A}*) and 802 (*mak-2::hph; his3::Ptef-1–mak-2^{Q100A}–gfp*) in the presence of DMSO 0.2% (control). (B) Cell interaction of spores of strains MAL-1 and 802 in the presence of 40 µM 1-NM-PP1. Inh, inhibitor. Scale bars: 5 µm. Comparable observations were made for multiple samples (*n*=5).

fungi (Takemoto et al., 2011). These complexes have an essential role for germling and hyphal fusion in this group of organisms (Dirschnabel et al., 2014; Roca et al., 2012). The potential link between NOX and MAPK signaling is currently strongly debated. We therefore asked whether the role of BEM-1 in germling and hyphal fusion, and potentially MAK-2 regulation, is NOX-related or independent. In a first step, we quantified the previously reported defects of the NOX-complex mutants Δ*nox-1*, Δ*ham-6* and the regulator mutant Δ*nor-1* (715). As expected from other organisms, the proteins NOX-1, NOR-1 and HAM-6 (also referred to as NOX-D) are essential for germling interactions (Fig. 8A). In the next step, MAK-2–GFP–CAAX was expressed in the Δ*bem-1*, Δ*nox-1*, Δ*ham-6* and Δ*nor-1* backgrounds, resulting in strains 569, 723, 773 and 719, respectively. Fluorescence microscopy showed that membrane tethering of *mak-2–gfp–caax* was not affected in any isolate (Fig. 8B). A potential defect in MAK-2 activation in these strains was analyzed by phospho-western blot analysis. Although MAPK hyperphosphorylation in the NOX mutants was similar to that in the wild type, no activation was detected in Δ*bem-1*, and reduced activation was detected in Δ*ham-6* (Fig. 2C,D). This finding strongly suggests that BEM-1 has a role in MAK-2 activation which is independent of its potential function in the NOX complex. The NOX complexes, however, function either downstream or independently of MAK-2 during germling and hyphal fusion, except for HAM-6 which has been hypothesized to be part of the cell wall integrity membrane sensor (Fu et al., 2014).

DISCUSSION

The cell communication process mediating somatic cell fusion in *N. crassa* provides an excellent model for studying the contribution of

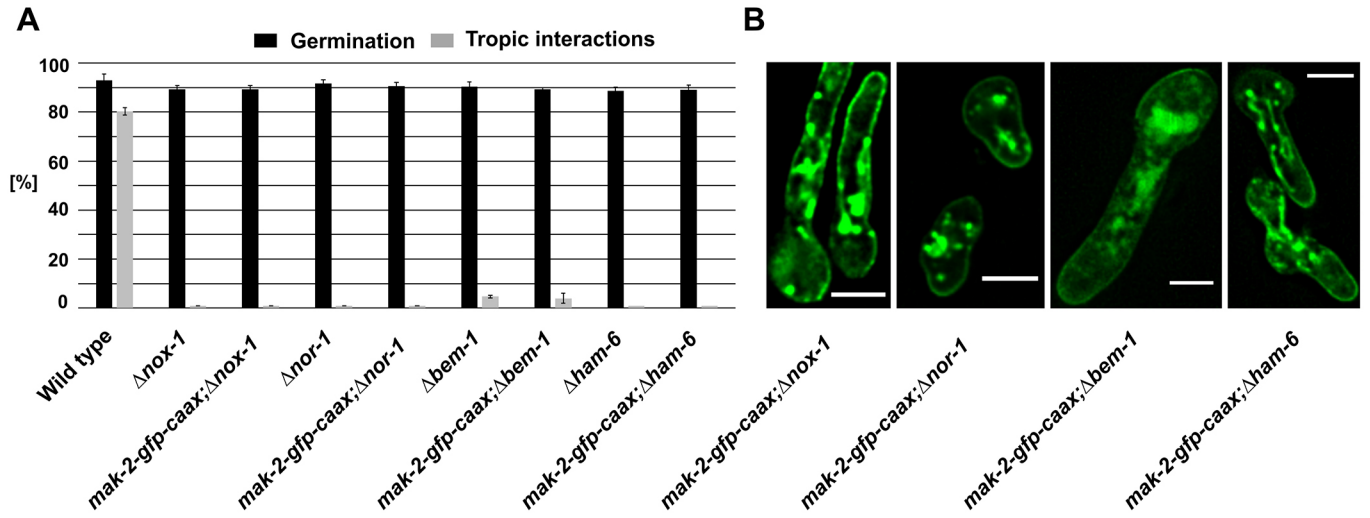

Fig. 8. NOX complex mutants are affected in their tropic interactions. (A) Quantification of tropic interactions 4 h post inoculation in the following strains: wild type (FGSC 2489), Δ*nox-1*, 723 (*nox-1::hph;his3::Ptef-1–mak-2–gfp–caax*), Δ*nor-1*, 719 (*nor-1::hph;his3::Ptef-1–mak-2–gfp–caax*), Δ*bem-1*, 569 (*bem-1::hph; his3::Ptef-1–mak-2–gfp–caax*), Δ*ham-6* and 773 (*ham-6::hph;his3::Ptef-1–mak-2–gfp–caax*). Results are means±s.d. (*n*≥100). (B) Localization of the membrane-tethered MAK-2 in different deletion mutants of the ROS generating system. Scale bars: 5 µm. Comparable observations were made for multiple samples (*n*≥5).

Journal of Cell Science (2018) 131, jcs213462. doi:10.1242/jcs.213462

spatial and temporal subcellular dynamics to MAPK regulation. In this study, we show that subcellular dynamics of the MAK-2 kinase are essential for coordination in the behavior of the fusion partners, and that these dynamics require and control the activation and function of the kinase. In addition, we describe a function of MAK-2 during cell-cell fusion that is independent of its role during tropic growth.

Spatio-temporal dynamics of MAK-2 are essential for its function during tropic growth

The permanent tethering of the kinase to the plasma membrane triggers its phosphorylation but results in a loss of function. A well-established role of MAPKs is the transmission of extracellular signals into the nucleus. Earlier studies have indicated that MAK-2 targets the transcription factors PP-1, RCO-1 and RCM-1 during germling interactions (Aldabbous et al., 2010; Fu et al., 2011; Liu et al., 2015). Although transcriptional reprogramming and *de novo* protein synthesis are not essential once the cell-cell interaction is established, both are necessary for initiating the process (Fleissner et al., 2009). Therefore, a failure of MAK-2 to translocate into the nucleus likely prevents the induction of the cellular interaction. Consistent with this hypothesis, membrane trapping of the upstream kinase MEK-2, which is always excluded from the nucleus, still allowed partial functioning of this process. This observation also suggests that MAK-2 translocates independently of the three-tiered kinase complex towards the nucleus. This finding contrasts with those in a report in *Aspergillus nidulans*, in which the homologous kinase module translocates as a complex to the nuclear envelope, when controlling differentiation and secondary metabolism (Bayram et al., 2012). It will, therefore, be of great interest to determine whether and how the different dynamics of the MAPK complexes reflect distinct functions in specific developmental contexts.

Expression of MAK-2–CAAX in the wild-type background resulted in reduced cellular interactions. In these cells, the SO protein failed to translocate to the plasma membrane. This effect, however, strongly depends on the activation state of MAK-2, such that a non-phosphorylatable variant has no negative effect on the interactions. Together, these observations provide a first indication of the functional relationship between the MAK-2 module and the SO protein. The alternating wild-type dynamics of these proteins likely require an intricate network of positive and negative regulatory feedback loops (Goryachev et al., 2012). Our data support a model in which recruitment of MAK-2 to the membrane positively reinforces its activation. Two opposite mechanisms might contribute to this effect. First, membrane recruitment might locally concentrate the kinase module and upstream activating factors, resulting in more efficient signal transduction. Earlier studies have shown that the activation depends on the interaction of the three kinases with the scaffold protein HAM-5 (Jonkers et al., 2014). In addition, our data indicate that the polarity factor BEM-1, which resides at the growing cell tips, also promotes MAK-2 activation and might link the general polarity machinery to the signaling cascade, resulting in directed growth towards the fusion partner. Second, membrane recruitment might separate the kinase from inactivating factors, including phosphatases. So far, the MAK-2-deactivating phosphatases remain unknown. In yeast, the MAK-2 homolog Fus3 is controlled by the phosphatases Msg5, Ptp2 and Ptp3, which reside in both cytoplasm and the nucleus (Zhan et al., 1997). Assuming similar localization patterns in *N. crassa*, membrane recruitment might efficiently separate these factors from their MAPK target.

The subcellular MAK-2 dynamics control but also depend on kinase activation and function

The dynamic alternating MAK-2 recruitment suggests that release from the plasma membrane must be triggered briefly after activation. Earlier studies on the scaffolding protein HAM-5 have suggested that MAK-2 phosphorylates the scaffold, resulting in complex disassembly (Dettmann et al., 2014; Jonkers et al., 2014). Consistent with this model, MAK-2 remained at the plasma membrane when inhibited, and the cells were arrested in their current stage. In the partner cell, in which MAK-2 resides in the cytoplasm, the kinase failed to translocate to the cell periphery. The observed dynamics are, therefore, not cell autonomous, but require the highly regulated interplay of both partners.

When expressed in the wild-type background, the MAK-2 variant carrying a mutation at the phosphorylation site T180 translocated to the plasma membrane, but was no longer released, resulting in the simultaneous presence of the kinase at both cell tips. MAPK phosphorylation is often mediated by a two-collision process through the active MAPK. The upstream kinase binds the MAPK, phosphorylates it once, and aligns the second phosphorylation site with its own active catalytic center. The subsequent second phosphorylation yields a fully activated MAPK. The first phosphorylation preferentially occurs at the tyrosine residue rather than the threonine residue (Ferrell and Bhatt, 1997). Our data suggest a similar mechanism of MAK-2 activation in *N. crassa*. Phosphorylation of the tyrosine residue is a prerequisite but is also sufficient for membrane recruitment in the wild-type background. Full phosphorylation is, however, essential for catalytic activity and release from the membrane, probably by phosphorylation of the scaffold, as mentioned above. A recent study analyzing the role of monophosphorylated Fus3 during yeast mating revealed a dominant-negative function of downregulating pathway activity. Appearance of the monophosphorylated kinase species is preceded by accumulation of the dual-phosphorylated variant, suggesting that dephosphorylation also contributes to the maintenance of both species pools (Nagiec et al., 2015). Based on our observations, we suggest that the different subcellular dynamics of the various phosphovariants as well as an impact on the turnover of the MAPK complexes might contribute to these findings.

MAK-2 has a function during cell-cell fusion which is independent from its role during tropic growth

After the two fusion partners have established physical contact, MAK-2 is recruited to and around the forming fusion pore. Interestingly, the dynamics and characteristics of this recruitment differ significantly from those at the tropic growth stage. After cell-cell contact, MAK-2 and SO colocalize, whereas their presence at the plasma membrane is mutually exclusive during tropic growth. Consistent with this notion, SO is also recruited to the fusion point in cells expressing the membrane-tethered MAK-2–CAAX version, which efficiently prevents SO recruitment before the cells touch. In addition, all of the tested MAK-2 phosphorylation site variants efficiently translocate to the fusion point, and inhibition of MAK-2 activity does not prevent this recruitment, in contrast to the behavior during tropic growth. Together, these data indicate that MAK-2 is efficiently recruited to the fusion point independently of its activation stage and its activity, suggesting different regulatory mechanisms compared with the tropic growth phase. A recent elegant study using the autocrine signaling cells of *Schizosaccharomyces pombe* revealed a tight link between MAPK-mediated pheromone signaling and the commitment to cell fusion, and this was independent of cell-cell contact (Dudin

et al., 2016). Although such a mechanism is also likely in *N. crassa*, our data clearly suggest that contact-mediated cell-cell signaling crucially influences MAK-2 dynamics. Consistent with this observation, one of our earlier studies identified a mutant that lacked this cell contact-mediated switch between tropic growth and cell-cell fusion. As a consequence, the germ tubes continue to tropically grow after cell-cell contact, resulting in corkscrew-like structures and fusion failure (Weichert et al., 2016). Interestingly, although MAK-2 inhibition does not prevent translocation of the kinase to the fusion point, it fully prevents cell-cell fusion, indicating that there is a critical enzymatic function of MAK-2 for the fusion process. Although in cell-cell communication, the kinase likely translates a secreted signaling ligand into directed growth, its function during cell-cell fusion remains more cryptic. Cell fusion requires a precise focusing of the fusion machinery to the point of pore formation. So far, the molecular composition of the fungal membrane fusion machinery is unknown. It is, however, likely that these fusion factors reach the plasma membrane via secretory vesicles. In *N. crassa*, vesicle assemblies orient themselves next to the forming fusion pore during hyphal fusion (Hickey et al., 2002). Similar observations have also been reported for myoblast fusion in *Drosophila melanogaster* (Önel et al., 2014). Transport and focusing of these vesicles likely involves the actin cytoskeleton, the assembly of which might be controlled by MAK-2, similar to its postulated role during tropic growth. In *S. pombe*, a formin-nucleated actin aster mediates the transport of cell wall-degrading hydrolases to the fusion point (Dudin et al., 2015), whereas in *S. cerevisiae*, the formin Bni1 is a direct target of the MAPK Fus3 (Matheos et al., 2004). Together, these observations strongly support a model in which signaling pathways that mediate polarization and tropic growth of the fusion cells also govern processes after cell-cell contact, resulting in cell-cell fusion. Future deciphering of the different dynamics and roles of MAPK at these different stages of the fusion process will, therefore, strongly enhance our understanding of sexual and somatic cell fusion.

MATERIALS AND METHODS

N. crassa strains and growth media

The strains used in this study are listed in the supplementary information (Table S1). Strains were generally grown in Vogel's minimal medium (VMM) (Vogel, 1956) supplemented with 2% sucrose as the carbon source and with 1.5% agar for solid media. Auxotrophic strains were grown in VMM with the required supplements. Homokaryons were purified by either single spore isolation (SSPi) or by crossing with wild type. For selection during SSPi, VMM with hygromycin (200 µg/ml) was used. Crosses were performed on Westergaard's medium as described previously (Westergaard and Mitchell, 1947). If not indicated otherwise, strains were incubated at 30°C.

Plasmid construction

The plasmid pEGFP-F corresponding to human c-Ha-Ras (GFP-F) was purchased from Clontech. The sequence encoding the GFP-F was amplified by PCR, purified by HiYield Gel/PCR DNA Fragment Extraction Kit (SLG) and cloned into the vector pMF272 (Freitag et al., 2004). To obtain the plasmid *pccg-1–gfp–caax*, *gfp* was amplified by PCR using the reverse primer 5′-AACCATGAATTCTCACATCATTATGCACTTGGCGCAGC-AGCCTGCTTGGACGTCCTCGTCACCGACGTCCATCTGCTTGTAC-AGCTCGTCCATGCCGAG-3′, which includes a sequence coding for the C-terminal 20 amino acids of the BAND protein. The PCR product was purified as described and cloned into the plasmid pMF272 using the restriction sites *Pac*I and *EcoR*I. In this plasmid, the promoter *pccg-1* was replaced by the *tef-1* promoter amplified from the plasmid pAB261 (Berepiki et al., 2010) using the forward-primer 5′-GGTGGCGGCCGCGATATCCCGTGACCACTGAACTACACTAG-TCAAGAGTGAAGCTTGTGG-3′. The resulting plasmid *ptef-1–gfp–caax* provided the basis for subsequent vector construction. The sequences coding for MAK-2 and MEK-2 were amplified as described previously (Dettmann et al., 2012) and integrated into the plasmid *ptef-1–gfp–caax* using restriction sites *Xba*I and *Pac*I, yielding the plasmids *ptef-1–mak-2–gfp–caax* and *ptef-1–mek-2–gfp–caax*. The sequences of *mak-2* and *mek-2* including their respective promoters were amplified by PCR as described earlier (Fleissner et al., 2009; Dettmann et al., 2012) and integrated into the plasmid *ptef-1–gfp–caax* using the restriction enzymes *Not*I and *Pac*I, therefore replacing the *tef-1* promoter. The resulting plasmids were *pmak-2–mak-2–gfp–caax* and *pmek-2–mek-2–gfp–caax*. To construct the plasmids containing the *gfp–saax* sequence, *gfp* was amplified using the reverse-primer 5′-AACCATGAATTCTCACATCATTATGGACTTGGCGGAG-GAGCCTGCTTGGACGTCCTCGTCACCGACGTCCATCTGCTTGTA-CAGCTCGTCCATGCCGAGA-3′ and integrated into the plasmid *ptef-1–gfp* using the restriction sites *Pac*I and *EcoR*I, replacing the original *gfp* sequence. Based on this plasmid, the plasmids *ptef-1–mak-2–gfp–saax*, *ptef-1–mek-2–gfp–saax* and *pmak-2–mak-2–gfp–saax* were constructed as described above for the respective *caax* plasmids.

Transformation

N. crassa strains were transformed by electroporation of macroconidia, according to a protocol previously described in Margolin et al., 1997.

Live-cell imaging

Sample preparation was performed as previously described (Schürg et al., 2012). Samples were observed on a Zeiss Observer 2.1 microscope using Nomarski optics with a Plan-Neofluar 100×/1.30 oil immersion objective (420493-9900) with an LED (CoolLED pE4000) as a light source for fluorescence microscopy. Images were captured with a PCO Edge 5.5 Gold (16 bit) camera controlled by a modified version of 4-D microscopy software programmed by Ralf Schnabel and Christian Hennig (Schnabel et al., 1997). Simple image analyses were performed with Fiji (ImageJ). Image stacks were obtained with an increment of 100 nm, and up to 10 focal stacks were captured. These stacks were deconvolved using Huygens deconvolution software (Scientific Volume Imaging), configuring default settings in classic mode with up to 100 iterations. To quantify the fluorescence intensity in interacting cells, a region covering an ∼3 µm distance from the cell tip was measured. The values were normalized to the fluorescence intensity detected in the cytoplasm 4-6 µm behind the cell tip (1 μm^2 was measured).

Quantitative phenotypic analysis

The phenotypical characterization of the strains included a quantification of aerial hyphal growth, germling fusion, growth rate and spore production, which were conducted as described previously (Schürg et al., 2012; Fleissner et al., 2009). Quantitative data were statistically analyzed by performing a two-tailed paired *t*-test using Excel.

Western blot analyses

To determine the level of MAPK phosphorylation in hyphae, strains were incubated in VMM for 3 days at 30°C (dark) and for 1 day at 26°C (12-h light–12-h dark). Fresh spores were harvested and filtered through cheesecloth. A total of 5×10^7 spores were inoculated in 50 ml of VMM in plastic flasks and incubated at 26°C with 120 rpm for 24 h. The mycelium was harvested by filtering through a layer of Miracloth (Calbiochem) and rapidly frozen in liquid nitrogen. Protein extraction and quantification was performed as previously described (Pandey et al., 2004). A total amount of 25 µg of protein per lane was separated on a sodium dodecyl sulfate (SDS) 8% polyacrylamide gel by electrophoresis (150 V) and transferred by wet blotting (Bio-Rad) onto PVDF membranes (Immobilon-P, 0.45 µm; Roth). Membranes were blocked by incubation in a 5% albumin fraction V, protease-free solution (Roth) for 12 h at 4°C. Membranes were washed three times for 5 min with 0.1% TBS-T (200 mM Tris-HCl pH 7.5, 1.5 M NaCl and 0.1% Tween-20) and incubated with antibody p44/42 MAPK (#9101 L, CST), diluted to 1:1000 with BSA for 12 h. After washing, membranes were incubated with a 1:120,000 dilution of the secondary antibody anti-rabbit

IgG, HRP-linked antibody (#7074, CST) at 4°C for 90 min. After washing with 0.1% TBS-T, membranes were developed with the SuperSignal West Femto (#34095, Thermo Fisher Scientific) chemiluminescence detection system (ChemiDoc MP, Bio-Rad). MAK-2 activation in germlings was tested using cellophane plates; 6×10^7 spores were inoculated per plate (10 plates per time point), incubated and rapidly frozen in liquid nitrogen. Protein extraction and analysis were done as described above.

Chemical inhibition of MAPK activity

The ATP analog-sensitive variant of MAK-2 was constructed by mutating the gatekeeper amino acid residue Q100 into an alanine residue, as described before (Fleissner et al., 2009). Addition of the inhibitor (1-NM-PP1, TRC A603003) and analysis of the macroscopic and microscopic phenotypic consequences were conducted as previously described (Fleissner et al., 2009; Weichert et al., 2016).

Achnowledgements

We thank Hanna Lunding and Viola Goebel for help with constructing some of the strains used in this study. We greatly acknowledge use of materials generated by the project 'Functional analysis of a model filamentous fungus', which was supported by a National Institutes of Health grant (PO1 GM068087).

Competing interests

The authors declare no competing or financial interests.

Author contributions

Conceptualization: A.S., J.I., A. Letz, A.F.; Methodology: A.S., J.I., U.B., N.T., A. Letz, A. Lichius, N.R., A.F.; Validation: A.S., J.I., N.T., A. Letz, A.F.; Formal analysis: A.S., J.I., N.T., A. Letz, A.F.; Investigation: A.S., J.I., U.B., N.T., A. Letz, A.F.; Resources: A.S., J.I., U.B., N.T., A. Letz, A. Lichius, N.R., A.F.; Data curation: A.S., J.I., A. Letz, A.F.; Writing - original draft: A.S., J.I., A.F.; Writing - review & editing: A.S., J.I., U.B., N.T., A. Letz, A. Lichius, N.R., A.F.; Visualization: A.S., J.I., N.T., A.F.; Supervision: A.S., J.I., A.F.; Project administration: A.S., J.I., A.F.; Funding acquisition: A.F.

Funding

This work has been supported by funding from the Deutsche Forschungsgemeinschaft (FL706-2) to A.F., the European Commission (PITN-GA-2013-607963) to A.F. and N.D.R., and the Biotechnology and Biological Sciences Research Council (BB/E010741/1) to N.D.R. Deposited in PMC for release after 6 months.

Supplementary information

Supplementary information available online at
http://jcs.biologists.org/lookup/doi/10.1242/jcs.213462.supplemental

References

Aldabbous, M. S., Roca, M. G., Stout, A., Huang, I.-C., Read, N. D. and Free, S. J. (2010). The ham-5, rcm-1 and rco-1 genes regulate hyphal fusion in *Neurospora crassa*. *Microbiology* **156**, 2621-2629.

Atay, O. and Skotheim, J. M. (2017). Spatial and temporal signal processing and decision making by MAPK pathways. *J. Cell Biol.* 216, 317-330.

Bayram, Ö., Bayram, Ö. S., Ahmed, Y. L., Maruyama, J.-i., Valerius, O., Rizzoli, S. O., Ficner, R., Irniger, S. and Braus, G. H. (2012). The *Aspergillus nidulans* MAPK module AnSte11-Ste50-Ste7-Fus3 controls development and secondary metabolism. *PLoS Genet.* **8**, e1002816.

Belden, W. J., Larrondo, L. F., Froehlich, A. C., Shi, M., Chen, C., Loros, J. J. and Dunlap, J. C. (2007). The band mutation in *Neurospora crassa* is a dominant allele of ras-1 implicating RAS signaling in circadian output. *Genes Dev.* **21**, 1494-1505.

Berepiki, A., Lichius, A., Shoji, J. Y., Tilsner, J. and Read, N. D. (2010). F-actin dynamics in *Neurospora crassa*. *Eukaryot. Cell* **9**, 547-557.

Bishop, A. C., Ubersax, J. A., Petsch, D. T., Matheos, D. P., Gray, N. S., Blethrow, J., Shimizu, E., Tsien, J. Z., Schultz, P. G., Rose, M. D. et al. (2000). A chemical switch for inhibitor-sensitive alleles of any protein kinase. *Nature* **407**, 395-401.

Cargnello, M. and Roux, P. P. (2011). Activation and function of the MAPKs and their substrates, the MAPK-activated protein kinases. *Microbiol. Mol. Biol. Rev.* **75**, 50-83.

Chen, R. E., Patterson, J. C., Goupil, L. S. and Thorner, J. (2010). Dynamic localization of Fus3 mitogen-activated protein kinase is necessary to evoke appropriate responses and avoid cytotoxic effects. *Mol. Cell. Biol.* **30**, 4293-4307.

Conlon, P., Gelin-Licht, R., Ganesan, A., Zhang, J. and Levchenko, A. (2016). Single-cell dynamics and variability of MAPK activity in a yeast differentiation pathway. *Proc. Natl. Acad. Sci. USA* **113**, E5896-E5905.

Dettmann, A., Illgen, J., März, S., Schürg, T., Fleissner, A. and Seiler, S. (2012). The NDR kine scaffold HYM1/MO25 is essential for MAK2 MAP kine signaling in *Neurospora crassa*. *PLoS Genet.* **8**, e1002950.

Dettmann, A., Heilig, Y., Valerius, O., Ludwig, S. and Seiler, S. (2014). Fungal communication requires the MAK-2 pathway elements STE-20 and RAS-2, the NRC-1 adapter STE-50 and the MAP kinase scaffold HAM-5. *PLoS Genet.* **10**, e1004762.

Dirschnabel, D. E., Nowrousian, M., Cano-Domínguez, N., Aguirre, J., Teichert, I. and Kück, U. (2014). New insights into the roles of NADPH oxidases in sexual development and ascospore germination in *Sordaria macrospora*. *Genetics* **196**, 729-744.

Dudin, O., Bendezu, F. O., Groux, R., Laroche, T., Seitz, A. and Martin, S. G. (2015). A formin-nucleated actin aster concentrates cell wall hydrolases for cell fusion in fission yeast. *J. Cell Biol.* **208**, 897-911.

Dudin, O., Merlini, L. and Martin, S. G. (2016). Spatial focalization of pheromone/MAPK signaling triggers commitment to cell – cell fusion. *Genes Dev.* **30**, 2226-2239.

Ferrell, J. E. and Bhatt, R. R. (1997). Mechanistics of the dual phosphorylation of mitogen- activated protein kinase. *J. Biol. Chem.* **272**, 19008-19016.

Fleissner, A., Leeder, A. C., Roca, M. G., Read, N. D. and Glass, N. L. (2009). Oscillatory recruitment of signaling proteins to cell tips promotes coordinated behavior during cell fusion. *Proc. Natl. Acad. Sci. USA* **106**, 19387-19392.

Fleißner, A. and Herzog, S. (2016). Signal exchange and integration during self-fusion in filamentous fungi. *Semin. Cell Dev. Biol.* **57**, 76-83.

Fleißner, A. and Serrano, A. (2016). The Art of Networking: Vegetative Hyphal Fusion in Filamentous Ascomycete Fungi. In: Wendland J. (eds) *Growth, Differentiation and Sexuality*. The Mycota (A Comprehensive Treatise on Fungi as Experimental Systems for Basic and Applied Research), vol I., pp 133-153, Springer, Cham.

Freitag, M., Hickey, P. C., Raju, N. B., Selker, E. U. and Read, N. D. (2004). GFP as a tool to analyze the organization, dynamics and function of nuclei and microtubules in *Neurospora crassa*. *Fungal. Genet. Biol.* **41**, 897-910.

Fu, C., Iyer, P., Herkal, A., Abdullah, J., Stout, A. and Free, S. J. (2011). Identification and characterization of genes required for cell-to-cell fusion in *Neurospora crassa*. *Eukaryot. Cell* **10**, 1100-1109.

Fu, C., Ao, J., Dettmann, A., Seiler, S. and Free, S. J. (2014). Characterization of the *Neurospora crassa* cell fusion proteins, HAM-6, HAM-7, HAM-8, HAM-9, HAM-10, AMPH-1 and WHI-2. *PLoS ONE* **9**, e107773.

Glass, N. L., Rasmussen, C., Roca, M. G. and Read, N. D. (2004). Hyphal homing, fusion and mycelial interconnectedness. *Trends Microbiol.* **12**, 135-141.

Good, M., Tang, G., Singleton, J., Reményi, A. and Lim, W. A. (2009). Scaffold-assisted catalysis: a novel domain in the Ste5 scaffold protein is required to unlock the MAPK Fus3 for phosphorylation by the MAPKK Ste7. *Cell* **136**, 1085-1097.

Goryachev, A. B., Lichius, A., Wright, G. D. and Read, N. D. (2012). Excitable behavior can explain the "ping-pong" mode of communication between cells using the same chemoattractant. *BioEssays* **34**, 259-266.

Harding, A., Tian, T., Westbury, E., Frische, E. and Hancock, J. F. (2005). Subcellular localization determines MAP kinase signal output. *Curr. Biol.* **15**, 869-873.

Hickey, P. C., Jacobson, D. J., Read, N. D. and Louise Glass, N. (2002). Live-cell imaging of vegetative hyphal fusion in *Neurospora crassa*. *Fungal Genet. Biol.* **37**, 109-119.

Hutchison, E., Brown, S., Tian, C. and Glass, N. L. (2009). Transcriptional profiling and functional analysis of heterokaryon incompatibility in *Neurospora crassa* reveals that reactive oxygen species, but not metacaspases, are sociated with programmed cell death. *Microbiology* **155**, 3957-3970.

Jonkers, W., Leeder, A. C., Ansong, C., Wang, Y., Yang, F., Starr, T. L., Camp, D. G., Smith, R. D. and Glass, N. L. (2014). HAM-5 functions as a MAP kinase scaffold during cell fusion in *Neurospora crassa*. *PLoS Genet.* **10**, e1004783.

Keshet, Y. and Seger, R. (2010). The MAP kinase signaling cascades: a system of hundreds of components regulates a diverse array of physiological functions. *Methods Mol. Biol.* **661**, 3-38.

Lamson, R. E., Takahashi, S., Winters, M. J. and Pryciak, P. M. (2006). Dual role for membrane localization in yeast MAP kinase cascade activation and its contribution to signaling fidelity. *Curr. Biol.* **16**, 618-623.

Leeder, A. C., Palma-Guerrero, J. and Glass, N. L. (2011). The social network: deciphering fungal language. *Nat. Rev. Microbiol.* **9**, 440-451.

Leeder, A. C., Jonkers, W., Li, J. and Glass, N. L. (2013). Early colony establishment in *Neurospora crassa* requires a MAP kinase regulatory network. *Genetics* **195**, 883-898.

Li, D., Bobrowicz, P., Wilkinson, H. H. and Ebbole, D. J. (2005). A mitogen-activated protein kinase pathway essential for mating and contributing to vegetative growth in *Neurospora crassa*. *Genetics* **170**, 1091-1104.

Li, Y., Roberts, J., Aghdam, Z. A. and Hao, N. (2017). Mitogen-activated protein kinase (MAPK) dynamics determine cell fate in the yeast mating response. *J. Biol. Chem.* **292**, 20354-20361.

Liu, X., Li, H., Liu, Q., Niu, Y., Hu, Q., Deng, H., Cha, J., Wang, Y., Liu, Y. and He, Q. (2015). Role for protein kinase a in the neurospora circadian clock by regulating white collar-independent *frequency* transcription through phosphorylation of RCM-1. *Mol. Cell. Biol.* **35**, 2088-2102.

Lyons, D. M., Mahanty, S. K., Choi, K., Manandhar, M. and Elion, E. A. (1996). The SH3-domain protein Bem1 coordinates mitogen-activated protein kinase cascade activation with cell cycle control in *Saccharomyces cerevisiae*. *Mol. Cell. Biol.* **16**, 4095-4106.

Maeder, C. I., Hink, M. A., Kinkhabwala, A., Mayr, R., Bastiaens, P. I. H. and Knop, M. (2007). Spatial regulation of Fus3 MAP kinase activity through a reaction-diffusion mechanism in yeast pheromone signalling. *Nat. Cell Biol.* **9**, 1319-1326.

Margolin, B. S., Freitag, M. and Selker, E. U. (1997). Improved plasmids for gene targeting at the his-3 locus of *Neurospora crassa* by electroporation. *Fungal Genet. Newsl.* **44**, 34-36.

Matheos, D., Metodiev, M., Muller, E., Stone, D. and Rose, M. D. (2004). Pheromone-induced polarization is dependent on the Fus3p MAPK acting through the formin Bni1p. *J. Cell Biol.* **165**, 99-109.

Merlini, L., Dudin, O. and Martin, S. G. (2013). Mate and fuse: how yeast cells do it. *Open Biol.* **3**, 130008-130008.

Nagiec, M. J., McCarter, P. C., Kelley, J. B., Dixit, G., Elston, T. C. and Dohlman, H. G. (2015). Signal inhibition by a dynamically regulated pool of monophosphorylated MAPK. *Mol. Biol. Cell* **26**, 3359-3371.

Önel, S. F., Rust, M. B., Jacob, R. and Renkawitz-Pohl, R. (2014). Tethering membrane fusion: common and different players in myoblasts and at the synapse. *J. Neurogenet.* **28**, 302-315.

Pandey, A., Roca, M. G., Read, N. D. and Glass, N. L. (2004). Role of a mitogen-activated protein kinase pathway during conidial germination and hyphal fusion in *Neurospora crassa*. *Eukaryot. Cell* **3**, 348-358.

Plotnikov, A., Flores, K., Maik-Rachline, G., Zehorai, E., Kapri-Pardes, E., Berti, D. A., Hanoch, T., Besser, M. J. and Seger, R. (2015). The nuclear translocation of ERK1/2 as an anticancer target. *Nat. Commun.* **6**, 6685.

Roca, G. M., Weichert, M., Siegmund, U., Tudzynski, P. and Fleißner, A. (2012). Germling fusion via conidial anastomosis tubes in the grey mould *Botrytis cinerea* requires NADPH oxidase activity. *Fungal Biol.* **116**, 379-387.

Schnabel, R., Hutter, H., Moerman, D. and Schnabel, H. (1997). Assessing normal embryogenesis in *Caenorhabditis elegans* using a 4D microscope: variability of development and regional specification. *Dev. Biol.* **184**, 234-265.

Schürg, T., Brandt, U., Adis, C. and Fleißner, A. (2012). The *Saccharomyces cerevisiae* BEM1 homologue in *Neurospora crassa* promotes co-ordinated cell behaviour resulting in cell fusion. *Mol. Microbiol.* **86**, 349-366.

Serrano, A., Hammadeh, H. H., Herzog, S., Illgen, J., Schumann, M. R., Weichert, M. and Fleißner, A. (2017). The dynamics of signal complex formation mediating germling fusion in *Neurospora crassa*. *Fungal Genet. Biol.* **101**, 31-33.

Takemoto, D., Kamakura, S., Saikia, S., Becker, Y., Wrenn, R., Tanaka, A., Sumimoto, H. and Scott, B. (2011). Polarity proteins Bem1 and Cdc24 are components of the filamentous fungal NADPH oxidase complex. *Proc. Natl. Acad. Sci. USA* **108**, 2861-2866.

van Drogen, F., Stucke, V. M., Jorritsma, G. and Peter, M. (2001). MAP kinase dynamics in response to pheromones in budding yeast. *Nat. Cell Biol.* **3**, 1051-1059.

Wainstein, E. and Seger, R. (2016). The dynamic subcellular localization of ERK: mechanisms of translocation and role in various organelles. *Curr. Opin. Cell Biol.* **39**, 15-20.

Weichert, M., Lichius, A., Priegnitz, B.-E., Brandt, U., Gottschalk, J., Nawrath, T., Groenhagen, U., Read, N. D., Schulz, S. and Fleißner, A. (2016). Accumulation of specific sterol precursors targets a MAP kinase cascade mediating cell–cell recognition and fusion. *Proc. Natl. Acad. Sci. USA* **113**, 201610527.

Westergaard, M. and Mitchell, H. K. (1947). Neurospora V. A Synthetic Medium Favoring Sexual Reproduction. *Am. J. Bot.* **34**, 573-577.

Vogel, H. J. (1956). A convenient growth medium for *Neurospora crassa*. *Microbial Genet. Bull.* **13**, 42-47.

Zhan, X., Deschenes, R. J. and Kun-liang, G. (1997). Differential regulation of FUS3 MAP kinase by tyrosine-specificphosphatases in *Saccharomyces cerevisiae*. *Genes Dev.* **11**, 1690-1702.